Journal of Thermal Analysis, Vol. 37 (1991) 2143-2164

THE MEASUREMENT OF IGNITION TEMPERATURES AND EXTENTS OF REACTION ON IRON AND IRON-NICKEL SULFIDES

J. G. Dunn and L. C. Mackey

SCHOOL OF APPLIED CHEMISTRY, CURTIN UNIVERSITY OF TECHNOLOGY, PERTH, WESTERN AUSTRALIA

Four mineral sulfides typically found in the feed stock of a commercial nickel flash smelter, namely pyrite, violarite, pyrrhotite and pentlandite, were isolated from a primary and a supergene ore sample using magnetic separation. Relatively pure samples of pyrite, pyrrhotite and pentlandite were obtained, but violarite could only be upgraded to a 40-50% mixture with pyrite. These samples were characterized by chemical analysis, optical microscopy, Electron Probe Microanalysis (EPMA), Scanning Electron Microscopy (SEM), X-ray Diffraction (XRD) and Thermogravimetry-Differential Thermal Analysis (TG-DTA). Each sample was split into four fractions of particle size 20–45 μm, 45–75 μm, 75–90 μm and 90–125 μm. Ignition temperatures and extents of reaction were determined using an isothermal thermogravimeter, and the products were characterized by electron microscopy. Pyrite and violarite were found to be the most reactive to ignition, followed by pyrrhotite, with pentlandite being the least reactive. This order contradicts the results of other studies and various possible causes for this are discussed. The observed trend of increasing ignition temperature with increasing particle size was in agreement with previously published reports. The extent of reaction of each mineral was measured at increasing furnace preheat temperatures. These plots were correlated with the morphology of the products formed at the ignition temperature.

Introduction

Flash smelting is a process widely used as a means of upgrading sulfide concentrates to produce a matte grade product. Although the technique was developed for copper sulfide melting, it has since been applied to other materials, including nickel sulfide. In Western Australia (WA), Western Mining Cooperation operates a nickel flash smelter at Kalgoorlie. Sulfide ore is mined in the surrounding regions, concentrated and then fed to the smelter. This concentrate comprises a mixture of iron and iron-nickel sulfide minerals, the primary constituents being pyrite, FeS_2; pyrrhotite, $Fe_{1-n}S$,

John Wiley & Sons, Limited, Chichester
Akadémiai Kiadó, Budapest

where $0<n<0.125$; pentlandite, $(FeNi)_9S_8$; and violarite, Ni_2FeS_4. The ideal stoichiometric formulae are given, but in practice considerable variation can occur. These materials are fed into the top of the reaction shaft under conditions sufficient to cause flash melting. This reaction occurs by an ignition mechanism.

Two important parameters in the study of ignition reactions are:

(i) the ignition temperature, which is defined as the minimum temperature required to cause a sufficient heating gradient to initiate an ignition reaction. It has been pointed out that this value is not a thermodynamic constant, and will vary with experimental conditions [1]

(ii) the extent of reaction (oxidation) of the mineral sulfide at various temperatures.

Several different methods for measuring the ignition characteristics of a sample have been employed, producing a considerable variation in results for what are ostensibly the same minerals [1–4]. Although some of the variation may be due to the different measurement techniques, there other reasons for discrepancies. For example, an important consideration is the stoichiometry of the mineral. It has been recently demonstrated that variation in the stoichiometry of pyrrhotite from $Fe_{0.83}S$ to FeS produces a change in ignition temperature of 200° [5]. Hence specification of the mineral by class alone is insufficient to reflect its tendency to ignite.

The aim of this work was to examine the ignition behaviour of the iron and iron-nickel sulfide minerals which comprise the feed to the Kalgoorlie Nickel Smelter. In addition to ascertaining the relative levels of reactivity and axplaining the observed trends with the support of SEM evidence, there was another important purpose to this work, namely to investigate other factors associated with natural minerals which might affect their reactivity, and to assess the importance of sample characterization procedures in assisting in making valid comparisons between data.

Experimental

Samples

The starting materials for this work were two sulfide samples:

(i) A supergene ore from the Rocky's open pit operation at Leinster, WA.

(ii) A primary ore from the Kambalda region, WA.

A polished section of each sample was prepared and examined under reflected light using a Zeiss Microscope to identify all of the phases present. The samples were then reduced in size using a hand pulverizer followed by an alumina disk grinder. The plate separation in the grinder was set at 1 mm. Further grinding was performed by hand with an agate mortar and pestle. The resulting material was sieved to collect the 45–125 μm fraction.

Magnetic separation methods

It was necessary to employ magnetic separation to obtain samples of pyrite, violarite, pyrrhotite and pentlandite from the two ore samples. The ferromagnetic nature of pyrrhotite allowed it to be separated from the primary ore using a hand magnet. A Frantz Magnetic Separator was utilized for further upgrading. The 45–125 μm samples were sieved at 45 μm in ethanol to remove any adhering fines and then dried.

The Frantz separator was operated at a constant forward slope of 25° on the vibrating chute. The current through the magnet and the side slope on the chute were varied. After pyrrhotite removal, the primary ore sample was processed at a current setting of 0.4 Å and a slope of 10°. The material responding in the magnetic fraction at this setting comprised the pentlandite sample. The pyrite-violarite sample was processed at 0.6 Å and 5°. The non-magnetic fraction was then run at 0.8 Å and 5°, the magnetic fraction at this second setting being collected was further processed at 1.5 Å, 10°, the non-magnetics at this setting being collected as pyrite.

Once samples had been upgraded a representative subsample of each was separated out, the remaining material being dry sieved to collect the following fractions: 45–75 μm, 75–90 μm and 90–125 μm. Some of the 90–125 μm fraction was ground to pass a 45 μm sieve. This material was then wet sieved in ethanol at 20 μm, a 20–45 μm fraction being collected and dried. Wet sieving was not possible for the ferromagnetic pyrrhotite as it could not be dispersed. Hence, a sub 45 μm fraction was collected. All samples were stored in a desiccator under vacuum as the supergene ore, in particular, is very susceptible to oxidation.

Characterization techniques

Iron, nickel and sulphur were determined by wet chemical techniques.

XRD analyses were performed on a Siemens D500 X-Ray Diffractometer by the X-Ray Analysis Laboratory in the Department of Applied physics at Curtin University.

Polished sections of the unreacted and reacted samples were examined using a Jeol JSM–35C Scanning Electron Microscope equipped with an energy dispersive spectrometer.

Photomicrographs were taken using the Robinson backscattered electron detector.

EPMA was performed on carbon coated polished sections using a Cameca SX–50 Electron Probe and wavelength dispersive spectrometers. Data was processed by ANU/CSIRO WANU–SX Software V7.03. Analyses were performed at an accelerating voltage of 25 kV and a beam current of 30 nÅ. Pyrite and nickel metal standards were employed. A count time of 20 seconds was used for iron and nickel, 40 seconds being used for sulphur. Approximately 20 particles in each sample were analysed.

BET surface area measurements were performed by the Particle Analysis Facility at Curtin University.

Thermal Analysis techniques were utilized in two separate modes for the study of oxidation reactions as follows:

(i) Simultaneous thermogravimetric-differential thermal analysis (TG-DTA) experiments were performed using a Stanton Redcroft Model 781 TG-DTA. Approximately 3–5 mg of sample was weighed into an alumina crucible, placed inside the furnace and heated at 10 deg/min to a maximum temperature of 1000° in an air atmosphere (30 $ml \cdot min^{-1}$). This mode of operation was primarily used as a characterization technique for the sulphide samples.

(ii) An isothermal TG technique used to simulate the rapid heating rates required for ignition has been previously documented [2]. Experiments were conducted in a Stanton Redcroft Model TG–750, together with a 5 mg sample and an oxygen atmosphere. The maximum furnace temperature was 900°.

Isothermal TG was used to identify the ignition temperature of the samples. The magnitude of the weight loss observed for a sample at any given temperature was directly proportional to the extent of reaction of the sample at that temperature. A value was calculated for this term as follows, assuming that by 900° all of the oxidable material had reacted.

$$\% \text{ Extent of reaction} = \frac{100 \text{ (weight loss at temperature T °C)}}{\text{(weight loss at 900 °C)}}$$

Results and discussion

Characterization of the ores and subsequent upgrading

Figure 1 shows an optical micrograph of the polished section of the primary ore sample. This ore was predominately comprised of pentlandite (Pn) and pyrrhotite (Po). Some chalcopyrite, primary pyrite and a small amount of spinel were also present. Under reflected light, pentlandite is easily distinguished from pyrrhotite by its yellow-gold colour, compared with the more pink hue of pyrrhotite. Another distinguishing feature is the octahedral cleavage exhibited by pentlandite. This characteristic allows pentlandite to be distinguished from primary pyrite, which is similar in colour.

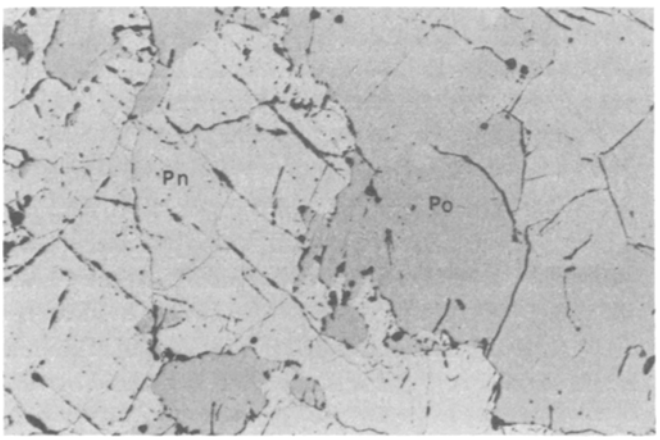

Fig. 1 Optical micrograph of a polished section of primary ore containing pentlandite and pyrrhotite as the major sulfide phases. Frame width = 2200 μm. Pn = pentlandite, Po = pyrrhotite

Magnetic separation of the primary ore was uncomplicated. The ferromagnetic pyrrhotite was easily removed by a hand magnet. It is likely that some material would have been physically entrained with the pyrrhotite, however, XRD results indicated that no significant quantities of any other phase were present. Frantz magnetic separation isolated a pure pentlandite sample, this being confirmed by XRD. The discarded non-magnetic fraction was examined using the EDS detector on the SEM. This sample contained chalcopyrite and primary pyrite. Hence magnetic separation was very successful for the primary ore.

An optical micrograph of the secondary ore appears in Fig. 2. The major phases present in the sample were violarite (V_{pn} and V_{po}) and secondary pyrite (Py), both of which are very porous. Violarite is a violet-grey colour compared with the yellow colour of secondary pyrite. Some carbonate was present, this being the dark grey phase evident in Fig. 2. A small quantity of primary pyrite was also identified. This is readily distinguished from the secondary mineral by its lack of porosity. Violarite predominatly occurred in the blocky formation shown on the left side of Fig. 2 (V_{pn}). This has resulted from pentlandite alteration and it is porous due to the associated volume reduction. The violarite- pyrite assemblage is known to be a supergene alteration product of the primary ore [6, 7]. Alteration commences with the appearance of specks of violarite throughout the pentlandite grain. These specks grow until the entire grain has been replaced. This process is accompanied by a loss of iron and nickel, the number of sulphur atoms per unit volume being assumed constant, consequently violarite is very porous. This mineral also inherits the octahedral cleavage exhibited by pentlandite. Some of the iron released during alteration is thought to precipitate as a carbonate, hence it is likely that the grey phase in Fig. 2 is siderite [6].

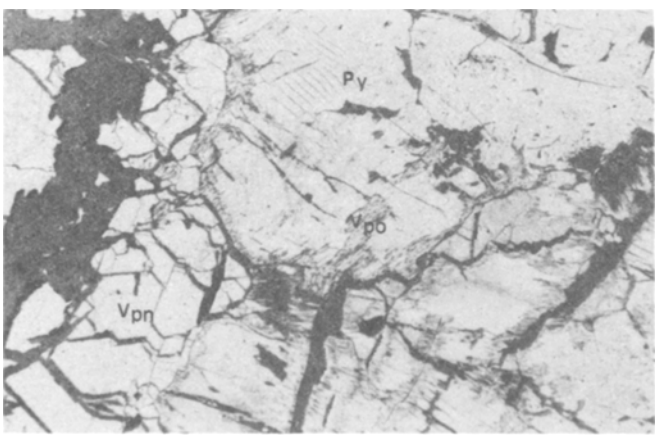

Fig. 2 Optical micrograph of a polished section of secondary ore containing violarite and pyrite as the major sulfide phases. Frame width = 1130 μm. Py = pyrite, V_{pn} = violarite (from pentlandite), V_{po} = violarite (from pyrrhotite)

A second type of violarite is observed in Fig. 2 (V_{po}). This 'fringed' or 'saw-tooth-like' phase was evident around the boundaries of the secondary pyrite. This mineral has formed by reaction of pyrrhotite with nickel released during the formation of violarite. The 'saw-tooth' appearance has been inherited from the twin lamellar structure of pyrrhotite [6]. This phase

is reported to be iron rich compared with the blocky form and is far less abundant due to the limited quantity of nickel available. Once all of the pentlandite has been consumed, pyrrhotite conversion to violarite ceases, due to the lack nickel. Secondary pyrite then forms. This is a result of the dissolution pf pyrrhotite, which is reprecipitated as pyrite, an iron less causing the pyrite to be porous. Deposition of layers of pyrite results in the colloform structure evident in the top of Fig. 2. Thus a secondary pyrite is distinguished readily from violarite by both structure and also by colour.

Table 1 Results of wet chemical analyses of the sulfide samples

Sample	Fe, %	Ni, %	S, %
Pyrite	37.5	–	44.8
Pyrrhotite	57.4	–	39.1
Pentlandite	29.6	35.0	33.2
Violarite	27.6	17.2	42.0

Magnetic separation of the pyrite-violarite sample presented some difficulties. While the primary pyrite in the pentlandite-pyrrhotite sample did not show any significant magnetic susceptibility, the secondary mineral responded over a wide range of settings. A pure sample of pyrite was readily obtained but it was not possible to isolate violarite. Extensive trials were conducted on the Frantz separator and the products were analysed by SEM-EDS in order to locate the setting yielding the maximum quantity of violarite. XRD analysis confirmed the presence of violarite and pyrite in this sample, together with some silica. The pyrite sample showed trace amounts of violarite by XRD analysis, some silica also being detected. However, in both the violarite and pyrite samples, marcasite was present. This mineral was not observed during the original examination of the supergene ore by optical microscopy. It would be easily distinguished from the chemically equivalent pyrite by anisotropy. Obviously the polished section was not representative of the bulk material. Marcasite is known to occur in violarite-pyrite assemblages [6], being porous and frequently colloform as is secondary pyrite. For the purpose of convenience in this paper, the pyrite-marcasite sample will be simply referred to as pyrite, while the violarite-pyrite mixture will be labelled violarite.

The results of wet chemical analysis on the bulk subsamples of the four sulfides are presented in Table 1. The pyrrhotite and pentlandite samples showed an analysis total of 96–98%, while the pyrite and violarite only totalled 82–87%. Some of this discrepancy was accounted for by silica and

carbonate. EPMA also indicated the presence of 1.5-2% of nickel within the pyrite particle on average, a maximum of 4% being measured. This agreed with EPMA results reported by Nickel *et al.* [6] for pyrite of a similar origin. Hence the solution from which pyrite was precipitated was obviously nickel enriched. 0.4–1% of nickel was also measured in the pyrrhotite sample. Once again, this agreed well with published data [6]. On the basis of the nickel content of the violarite-pyrite mixture, this sample is estimated to be 40–50% violarite.

Table 2 Stoichiometries of the sulfide minerals as determined by EPMA

Samples	Stoichometry
Pyrite	FeS_2
Pyrrhotite	$Fe_{0.85}S$
Pentlandite	$Ni_{4.90}Fe_{4.45}S_8$
Violarite	$Ni_{2.00}Fe_{1.05}S_4$

The average stoichiometry of each mineral, as calculated by EPMA of 20 particles, is given in Table 2. The results for pyrite and violarite are close to the previously stated theoretical stoichiometries. No iron rich violarite derived from pyrrhotite was detected in the 20 particles analysed. The pyrrhotite stoichiometry was slightly low compared with the results of XRD analysis. The latter indicated an iron:sulphur ratio of 0.875:1 which is consistent with monoclinic pyrrhotite. This agreed with the results reported in a previous study on Kambalda ore [6]. Hence, it seems likely that the EPMA data was approximately 1% in error. This could be due to the differences in structure and composition between the sulfide samples and the pyrite and nickel metal standards. The measured stoichiometry of pentlandite also seemed to be slightly in error, the iron value being higher than previously reported [6]. Values of the nickel:iron:sulphur ratio for the pentlandite samples examined in the two studies were 4.90 : 4.45 : 8 and 4.90 : 4.10 : 8 respectively. These discrepancies were not major.

SEM micrographs of polished sections of the 45–75 μm fraction of the samples are shown in Figs 3(a)–(d). All particles exhibited an angular shape.The pyrite particles (Fig. 3(a)) were porous and some showed the colloform structure. Pyrrhotite and pentlandite were very smooth in section (Figs 3(b) and 3(c)). However, both showed particle cracking, the pentlandite sample in particular being very fractured. This must have occurred during the grinding of the original ore sample. Cracking was not evident in either the pyrite or the violarite samples, yet all samples were subjected to

the same grinding process. The characteristic octahedral cleavage of pentlandite probably explains these observations. The reactivity of this mineral may be effected by the associated increase in surface area.

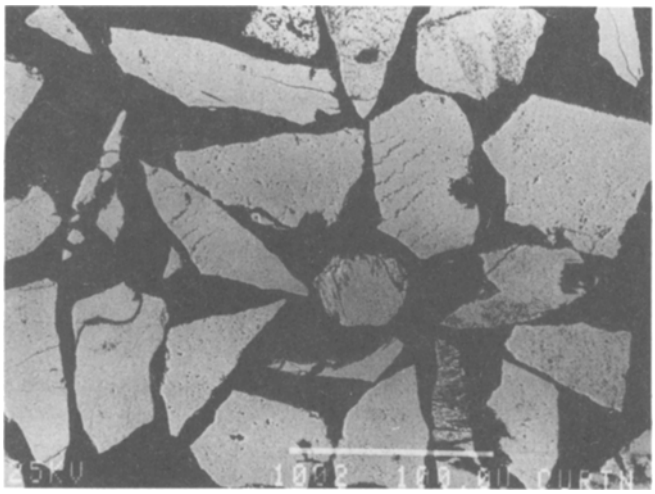

Fig. 3a Backscattered electron micrographs of the 45–75 μm fraction of unreacted pyrite

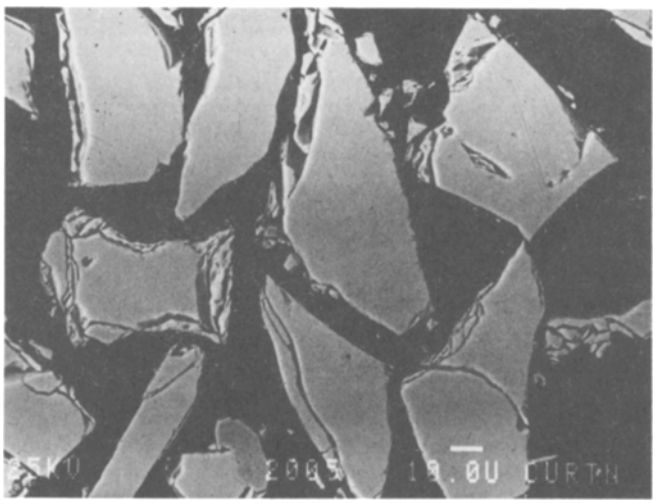

Fig. 3b Backscattered electron micrographs of the 45–75 μm fraction of unreacted pyrrhotite

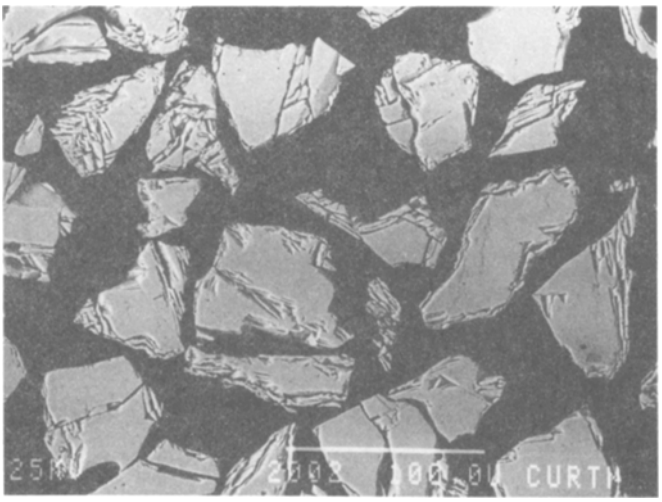

Fig. 3c Backscattered electron micrographs of the 45–75 μm fraction of unreacted pentlandite

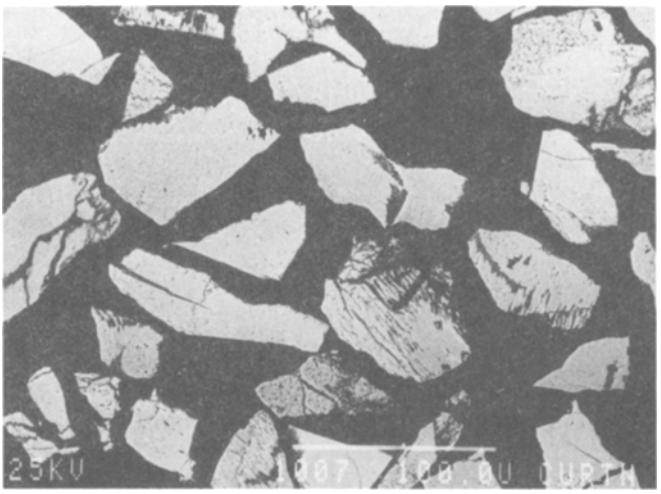

Fig. 3d Backscattered electron micrographs of the 45–75 μm fraction of unreacted violarite

Figure 3(d) shows the violarite sample. It is difficult to differentiate between the blocky violarite and secondary pyrite in this micrograph. The 'fringed', pyrrhotite-derived violarite, however, is readily identified.

TG–DTA studies

TG–DTA and ignition work were generally performed using the 45–75 μm size fraction of each sample. This fraction seemed most approximate to examine for reasons of handling convenience, but more importantly, because the feed supplied to the Kambalda nickel smelter is at least 80% finer than 75 μm.

Each sample was characterized using TG–DTA. The results are shown in Figs 4(a)–(d). Pyrrhotite has a characteristic endotherm at approximately 325–330° (Fig. 4(a)). This is caused by a transition in crystal structure from the monoclinic form to the hexagonal one [8]. This endotherm is valuable for detecting the presence of pyrrhotite. Note the absence of this peak in the DTA traces for the pentlandite, pyrite and violarite samples (Figs 4(b)–4(d)). Exothermic activity for pyrrhotite commenced at 480°, becoming more significant by 530° and continuing until 665°. A single mass loss of 13.5% was observed over this temperature range, a gradual loss of 2.5% continuing to 1000°.

Figure 4(b) shows that pentlandite experienced a 3% mass gain prior to the onset of significant exothermic activity and mass loss at approximately 590°. This gain in mass was attributed to the formation of iron and nickel sulphates. From this point onwards, the sample continued to lose mass in several stages. Endothermic effects evident to 795° have been attributed to sulfate decomposition [9, 10]. Iron(III) sulfate is reported to decompose above 550°, and nickel(II) sulfate decomposes slowly beyond 700°. A significant feature in the pentlandite DTA trace occurred at 795° with the appearance of a sharp endotherm which was followed immediately by an exotherm. It has been suggested that this combination is due to melting of an $Ni_{3\pm x}S_2$ phase followed by its oxidation [9].

In Fig. 4(c) the pyrite DTA trace showed slight exothermic activity from approximately 400°, the major exotherm being observed in the temperature range 450–540°. This was associated with a sharp mass loss, corresponding to 22% of the sample mass. A further loss of 8% occurred in the range 590–630° associated with a small endotherm. This is typical of iron(III) sulfate decomposition [10].

Exothermic activity for the violarite-pyrite mixture (Fig. 4(d)) commenced at 395°, finishing at 530°. This agreed fairly well with the temperature range for the pyrite sample, however, the presence of violarite increased the level of DTA activity prior to 450°. The mass loss associated with the exothermic effect was only 11%. A total loss of 26% was achieved in several stages. The first stage occurred in the range 585–625°, cor-

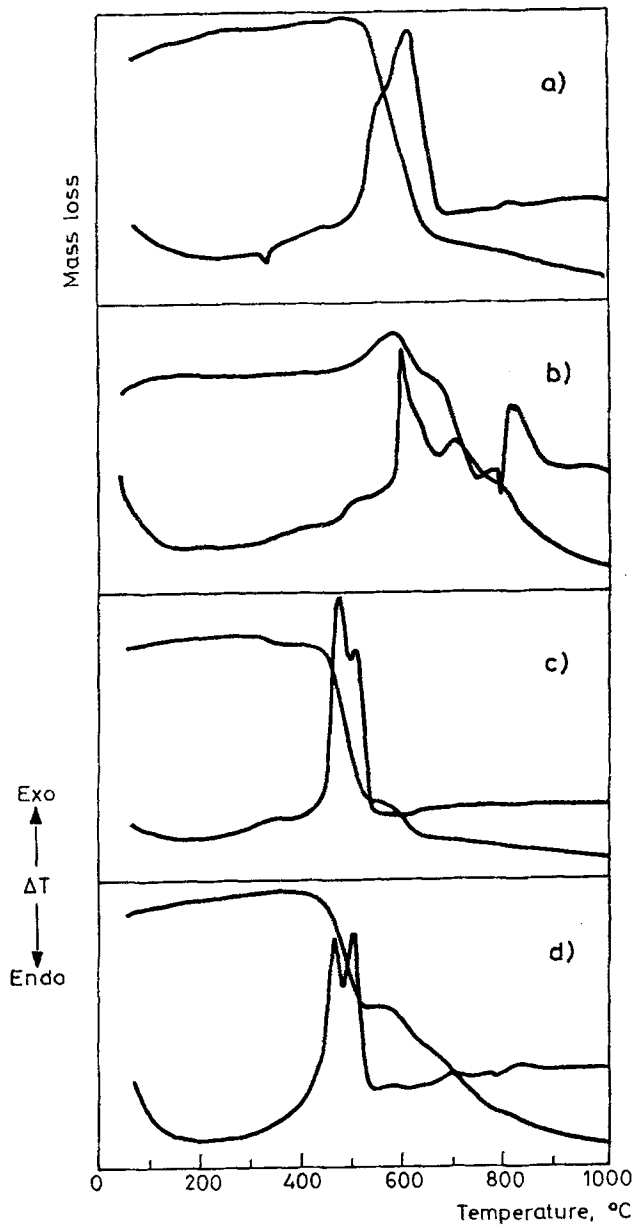

Fig. 4 TG–DTA record of the 45–75 μm fraction of sulfide samples heated at 10 deg·min^{-1} in air: (a) pyrrhotite, (b) pentlandite, (c) pyrite, (d) violarite

responding to the mass loss observed in the pyrite sample. Hence, this is attributed to iron(III) sulfate decomposition. The remaining loss is most likely caused by the decomposition of nickel(II) sulfate. The DTA activity above 530° was minimal, except for a small endothermic peak at 790°. This corresponds with observations for pentlandite, although the following exothermic effect was negligible. This endothermic peak was diagnostic for the two nickel sulphides. It should be noted that the overall activity for these two sulphides continued until at least 800° whereas pyrite and pyrrhotite had finished reaction by approximately 630 and 665° respectively.

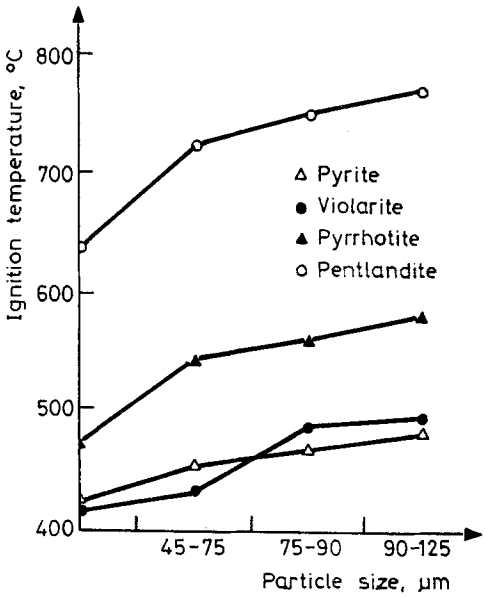

Fig. 5 Ignition temperatures of the sulfide samples as a function of particle size

In summary, pyrite and violarite completed their major exothermic oxidation reaction by approximately 530–540°. Pyrrhotite, however, did not commence significant oxidation until approximately 530°,and pentlandite not until 590°. The order of decreasing reactivity of the sulphides under these experimental conditions is:

pyrite, violarite > pyrrhotite > pentlandite

Ignition studies – particle size effects

The ignition temperatures of the four fractions of each of he sulfide samples as determined by isothermal TG are presented in Table 3 and Fig. 5. The ignition temperatures were determined from the temperature at which the first major mass loss occurred. These values are reproducible to within 5–10°. Note that the result in the 20–45 μm column for pyrrhotite actually represents the <45 μm fraction. Hence this value may be lower than would have been recorded for a 20–45 μm fraction due to the presence of a substantial amount of sub 20 μm material.

Table 3 Ignition temperatures of the sulfide size fractions as measured using isothermal TG

Mineral	Size fraction, μm			
	20–45	45–75	75–90	90–125
pyrite	420–425°C	450–455°C	465–470°C	478–483°C
violarite	412–417°C	430–435°C	482–487°C	490–495°C
pyrrhotite	470–475°C	540–545°C	555–560°C	575–580°C
pentlandite	635–640°C	720–725°C	745–750°C	765–770°C

Each mineral showed a definite trend to increasing ignition temperature with increasing particle size. The ignition temperatures for pyrite and violarite were within 20° of each other for all size fractions. Note that the violarite size fractions up to 75 μm ignited at a lower temperature than those of pyrite, while the trend was reversed for the larger particles. It is not reasonable to interpret these results in any depth since the reactivity of the violarite sample would have been influenced by the substantial quantity of pyrite present. However, it seems that the ignition temperature of violarite was more influenced by particle size than was that of pyrite. A 75° increase in ignition temperature was observed between the finest and coarsest fractions of violarite compared with a value of 60° for pyrite. The particle size effect caused an increase of 100 and 130° between the finest and coarsest fractions of pyrrhotite and pentlandite respectively. Hence the order of effect of particle size on ignition temperature was:

pyrite < violarite< pyrrhotite < pentlandite

The magnitude of the particle size effect measured for each sample and the relative trend was comparable with the results of a previous study [4].

Ignition studies – ignition temperatures

The ignition temperatures for the 45–75 μm fraction for violarite, pyrite pyrrhotite and pentlandite were 430–435, 450–455, 540–545 and 720–725°.

On this basis the order of ease of ignition is

$$\text{violarite} = \text{pyrite} < \text{pyrrhotite} < \text{pentlandite}$$

This observed order of reactivity matches that observed in the TG–DTA studies, but contradicts previous work which has found pyrite and violarite to be more reactive than pentlandite, with pyrrhotite being the least reactive [1, 4]. Previous studies have reported on the ignition behaviour of samples of these four minerals sourced from the Kambalda region using isothermal-TG [4]. The ignition temperatures of the 45–75 micron fractions were as follows: pyrite, 390–395°; violarite, 395–400°; pentlandite, 475–480°; and pyrrhotite, 495–500°. The results of the present study are, thus, between 35–60° higher than the previous set for violarite, pyrite and pyrrhotite, but in the case of pentlandite it is 250° higher. As the equipment used in both studies was identical, the source of these discrepancies must lie in the samples, their method of handling and the interpretation of results. Three possible sources of error can be suggested in the previous study:

(a) A different interpretation of what constitutes ignition. Whilst the other three sulfides have a definite weight loss and an overheating in the temperature trace at the ignition point, pentlandite exhibits overheating whilst showing a mass gain. Hence simultaneous sulfation and oxidation make it difficult to determine the ignition temperature with accuracy. In the present study the first definite weight loss was taken as the ignition temperature.

(b) The presence of fines adhering to the large particles, as a result of the use of the less efficient dry sieving technique.

(c) Contamination of the sample with more reactive sulfides.

The last two effects would result in a lowering of the observed ignition temperature.

The importance of thorough sample characterization procedures is readily apparent. A graphic illustration of this arose in the early stages of the current study in the search for pure minerals. Pyrite was readily obtained in a very pure form from the United Kingdom. The ignition temperature of the 45–75 μm was measured at 490–495°, which was 40° higher than the value for the supergene (secondary) pyrite sample. Wet chemical analysis and EPMA results on the two samples were essentially the same.

However, optical microscopy revealed that the UK pyrite was a primary mineral and consequently very dense compared with the porous secondary pyrite. Surface area measurements using a BET apparatus confirmed these observations, giving values of 0.6 m^2/g for the secondary sample compared with 0.1 m^2/g for the primary one. The lower ignition temperature of the secondary pyrite relative to the primary pyrite thus correlates with the greater surface area. This example stresses the importance of using samples of an appropriate geological origin to allow sensible comparisons.

The nature of the nickel sulphide deposits could explain some experimental discrepancies. As discussed earlier, pyrite and violarite are supergene alteration products of pentlandite and pyrrhotite. Obviously it was important to avoid samples from the transition area where partial replacement of the pentlandite and pyrrhotite has occurred. Care was also required in sample storage. Violarite and pyrite readily decompose when exposed to the atmosphere to form oxide and carbonate species [6, 7]. A ground, supposedly pure, violarite sample received for use in the current study was found to be ferromagnetic. Optical examination revealed the presence of thick rims of decomposition product, around the particles. Pitfalls such as these will only be avoided if characterization procedures are adequate.

Ignition studies – Extent of reaction curves and SEM evidence

Figures 6 and 7 show the extent of reaction plots for the 45–75 μm fraction of each sample with increasing preheat temperature of the furnace. Pyrite showed very little variation in the measured percent extent of reaction with increase in temperature. The trend for pyrrhotite was similar, although there was a slight temperature effect up to 650°. The observations for the pentlandite and violarite samples were markedly different. At the ignition point violarite exhibited 74% reaction. This value then increased in a regular manner with furnace preheat temperature. It is probable that this trend would have been even more pronounced had there not been a considerable quantity of pyrite present. The latter would elevate the measured extent of reaction. The extent of reaction for pentlandite showed a dramatic dependence on temperature. At the ignition point only 44% extent of reaction was measured.

Hence, these data confirm the observations of the TG–DTA studies that the behaviour of the iron sulfide minerals differs from that of iron-nickel sulfides. Once ignition is triggered in pyrite or pyrrhotite the thermal effect is sufficient to cause complete reaction, but this is not the case for violarite and pentlandite. In order to elucidate these trends the products collected at

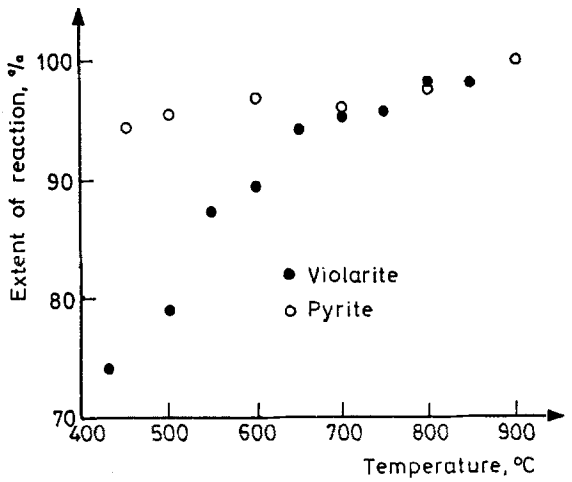

Fig. 6 Extent of reaction of the 45–75 μm fraction of pyrite and violarite-pyrite mixture at various reaction temperatures

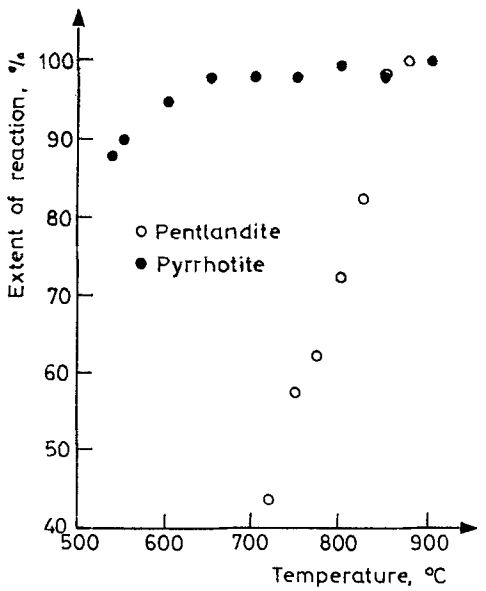

Fig. 7 Extent of reaction of the 45–75 μm fraction of pyrrhotite and pentlandite at various reaction temperatures

the ignition point were prepared as polished sections for SEM examination. Figures 8(a–d) show the resulting micrographs.

At the ignition temperature pyrite completely reacted to form a very porous product as seen from Fig. 8(a). This product was red in colour and

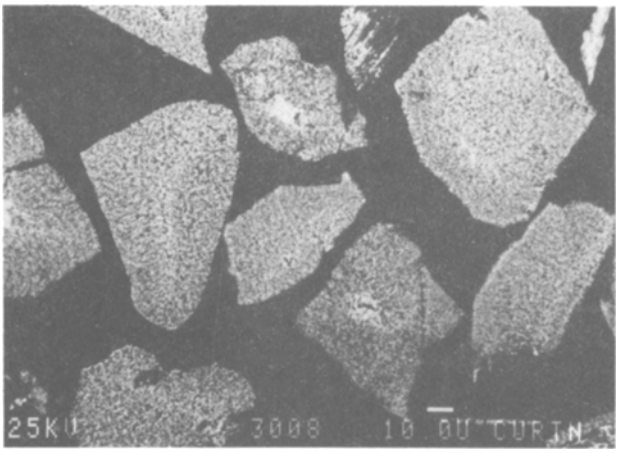

Fig. 8a Backscattered electron micrographs of the 45–75 μm fraction of pyrite just after ignition

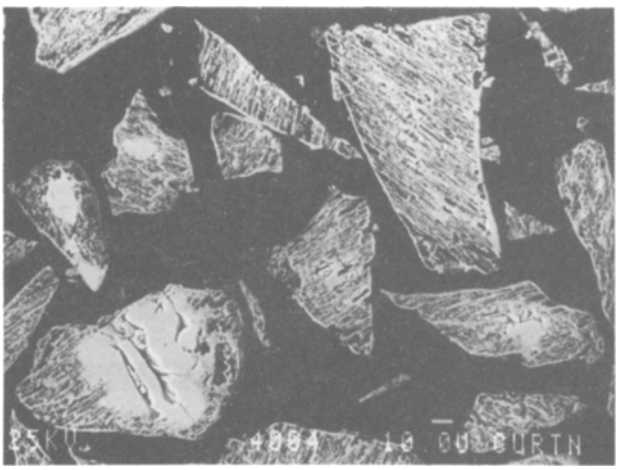

Fig. 8b Backscattered electron micrographs of the 45–75 μm fraction of pyrrhotite just after ignition

XRD evidence confirmed the presence of haematite. The observations for pyrrhotite were similar, the product analysing as haematite via XRD. Figure 8(b) shows that the ignited particles had a very porous appearance, but in contrast to pyrite these pores ran either along the length or across the width of the particle. The oxide has obviously inherited the fine lamellar twinning characteristic of pyrrhotite. This observation is supported by data

collected by Thornhill and Pidgeon [11] in a study of sulfide roasting. They reported that pyrrhotite appeared to oxidize preferentially along certain crystallographic planes. Note that some pyrrhotite grains in Fig. 8(b) contain areas of apparently unreacted sulfide. This would account for the slight temperature dependence of the extent of reaction curve up to 650°. Both small and large particles show unreacted material, hence this does not appear to be a particle size effect. It is likely that while the bulk of the sample completely oxidizes, some particles do not experience the necessary heating effects. However, raising the preheat temperature approximately 50–100° above the ignition point eliminates this effect.

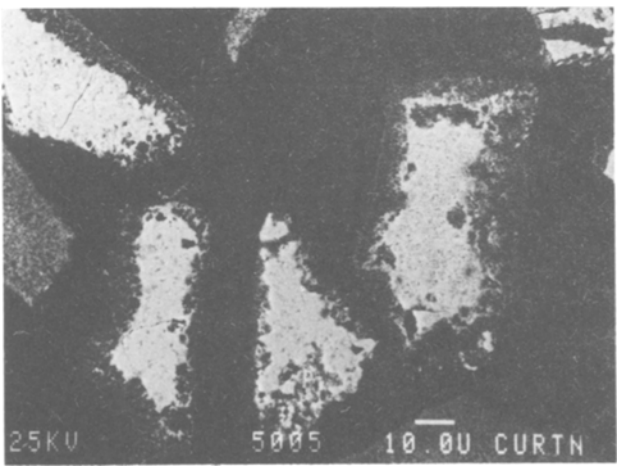

Fig. 8c Backscattered electron micrographs of the 45–75 μm fraction of violarite just after ignition

At the ignition temperature of violarite a rim of highly porous reaction product was evident surrounding an apparently unreacted core of sulphide (Fig. 8(c)). Approximately 20 particles of a sample ignited at 550° were examined using EPMA. This sample was used rather than that collected at the ignition point, so that a wider product rim was obtained for analysis. The results indicated that the rim was frequently an iron oxide with 5–10% of nickel present. XRD analysis confirmed the presence of haematite and perhaps magnesite. Some rims did, however, still contain higher levels of nickel and sulphur. A nickel sulphide species of approximate stoichiometry $Ni_{3.8}S_3$ was detected in the centre of many particles, a few percent of iron being present.

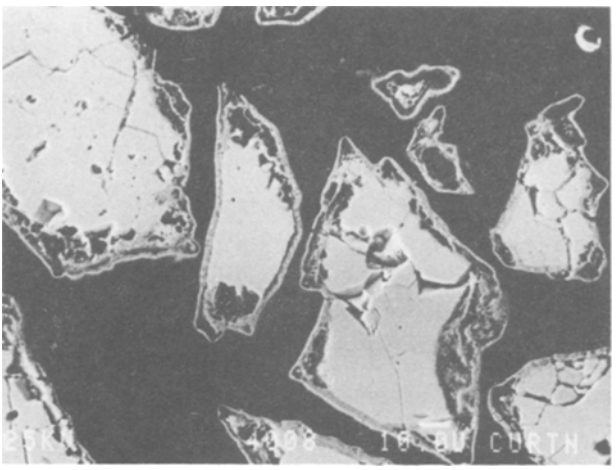

Fig. 8d Backscattered electron micrographs of the 45–75 μm fraction of pentlandite just after ignition

Pentlandite also exhibited a product rim surrounding an apparently unreacted core. However, in contrast to that observed for violarite, this rim was very dense (Fig. 8(d)). Porosity was evident on a larger scale, this being attributed to the cracked edges of the unreacted pentlandite particles. As mentioned earlier, this effect would be expected to enhance the reactivity of pentlandite due to the increase in surface area. The results of EPMA were similar to those for violarite. A sample ignited at 800° was examined. Results indicated the product rim to be iron oxide, with less nickel present on average than for violarite. XRD analysis confirmed the presence of haematite and magnesite. The particle centre was a nickel sulphide species of composition Ni_4S_3, a few percent of iron being detected. This was close to the stoichiometry of the violarite core, $Ni_{3.8}S_3$. The nickel contents of these phases are 71% and 70%respectively, and hence, the discrepancy is possibly due to analytical error in the EPMA data.

These observations account for the temperature dependence of the extents of reaction for violarite and pentlandite.

It is apparent that iron has migrated to the rim of both of the iron-nickel sulphides during the ignition process where it is preferentially oxidized, leaving behind a sulfide core enriched in nickel. This concept has been discussed in a report on sulfide roasting [11]. Pentlandite was observed to form an oxide shell surrounding a core of Ni_3S_2 and Ni_7S_6. These products were identified by XRD. The nickel contents of these phases are 73% and 68% respectively, compared with 70–71% nickel for the phases detected in the

current study. Hence, allowing for experimental error, these observations are comparable.

Conclusions

Magnetic separation has been successfully employed to separate pyrite, pyrrhotite and pentlandite from a complex nickel sulphide concentrate. A 40–50% upgrading of violarite was achieved. The ignition temperatures of pyrite, violarite and pyrrhotite were found to be similar to values reported in previous studies. The value for pentlandite was 250° higher than previously reported, and this caused a change in the order of reactivity to:

$$\text{violarite} = \text{pyrite} > \text{pyrrhotite} > \text{pentlandite}.$$

Increase in particle size caused an increase in the ignition temperature, this effect being most significant for pentlandite. SEM evidence indicated that pyrite and pyrrhotite reacted essentially to completion at the ignition temperature.

Pentlandite and violarite, however, showed preferential oxidation of iron in a product rim surrounding a core of nickel sulfide. The extent of reaction of the latter two minerals showed a marked dependence on temperature.

It is evident that considerable care needs to be taken in characterizing the samples, and that chemical analysis and XRD alone are insufficient to explain differences in the reactivity of the sulfides. The most important requirement is mineralogical assessment, in order to identify changes that have occurred in the sulfide since isolation from the source. Surface area measurements can also assist in explaining differences in reactivity.

* * *

We wish to express our thanks to Dr. R. Hill of the CSIRO Division of Exploration Geoscience, Perth, for providing the two ore samples used in this study. We are grateful for the use of CSIRO facilities, namely the electron probe and the sample polishing equipment. The assistance of several members of the above mentioned Division was most appreciated, in particular Drs E. Nickel, B. Robinson and Mr A. Bowyer. Finally, thanks are extended to Curtin University staff: Ms. J. Steer (XRD) and Associate Professor R. Pidgeon, Applied Geology (Frantz separation).

References

1 F. R. A. Jorgenson, Proc. Australas. Inst. Min. Metall., 268 (1978) 47.
2 J. G. Dunn, S. A. A. Jayaweera and S. G. Davies, Bull. Proc. Australas. Inst. Min. Metall., 290(4) (1985) 75.
3 J. G. Dunn, T. N. Smith, I. R. Stevenson and L. C. Mackey, Proc. 15th Australes, Chem. Eng. Conf., Melbourne, Vol.2, 1987, p. 101.
4 J. G. Dunn, S. G. Davies and L. C. Mackey, Proc. Australas. Inst. Min. Metall., 294(6) (1989) 57.
5 J. G. Dunn and A. Chamberlain, Thermochim. Acta, in press.
6 E. H. Nickel, J. R. Ross, and M. R. Thornber, Econ. Geol., 69 (1974) 93.
7 E. H. Nickel, P. D. Allchurch, M. G. Mason and J. R. Wilmshurst, Econ. Geol., 72 (1977) 184.
8 W. A. Deer, R. A. Howie and J. Zussman, Rock-Forming Minerals, Vol. 5, Non-Silicates, Longmans, London 1962, p. 146.
9 J. G. Dunn and C. E. Kelly, J. Thermal Anal., 18 (1980) 147.
10 J. G. Dunn, G. C. De and B. H. O'Connor, Thermochim. Acta, 145 (1989) 115.
11 P. G. Thornhill and L. M. Pidgeon, J. Metals, 9 (1957) 989.

Zusammenfassung — Mittels magnetischer Trennung wurden aus einer primären und einer supergenen Erzprobe vier Mineralsulfide, namentlich Pyrit, Violarit, Pyrrhotin und Pentlandit isoliert, die normalerweise im Einsatzmaterial eines kommerziellen Nickel-Schweberöstschmelzgerätes zu finden sind. Von Pyrit, Pyrrhotin und Pentlandit wurden relativ reine Proben erhalten, bei Violarit konnte als Mischung mit Pyrit nur ein Reinheitsgrad von 40-50 % erreicht werden. Diese Proben wurden mittels chemischer Analyse, optischer Mikroskopie, EPMA, Scanning-Elektronenmikroskopie, Röntgendiffraktion und TG-DTA beschrieben. Jede der Proben wurde in vier Fraktionen mit den Partikelgrößen 20-45m, 45-75m, 75-90m und 90-125m aufgespalten. Zündungstemperatur und Umsatzgrad der Reaktion wurden mittels einer isothermen thermogravimetrischen Methode bestimmt, die Produkte mittels Elektronenmikroskopie beschrieben. Bei der Entzündung zeigten sich Pyrit und Violarit als reaktionsfähigste Erze, gefolgt von Pyrrhotin und Pentlandit als am wenigstens reaktionsfähig. Diese Reihenfolge steht im Widerspruch zu den Ergebnissen anderer Studien und es werden verschiedene Ursachen diskutiert. Die beobachtete Tendenz, wonach mit steigender Partikelgröße auch die Entzündungstemperatur anwächst, steht in Übereinstimmung mit bereits veröffentlichen Untersuchungen. Der Umsatzgrad wurde für jedes Mineral bei steigender Ofenvorwärmtemperatur gemessen. Die Ergebnisse wurden mit der Morphologie der Reaktionsprodukte in Zusammenhang gebracht, die bei der Entzündungstemperatur entstehen.